01 Mar 2017

Estimating the Permanent Loss of Groundwater Storage in the Southern San Joaquin Valley, California

Ryan G. Smith
Missouri University of Science and Technology, smithryang@mst.edu

Rosemary Knight

J. Chen

J. A. Reeves

et. al. For a complete list of authors, see https://scholarsmine.mst.edu/geosci_geo_peteng_facwork/1363

Recommended Citation

R. G. Smith et al., "Estimating the Permanent Loss of Groundwater Storage in the Southern San Joaquin Valley, California," *Water Resources Research*, vol. 53, no. 3, pp. 2133-2148, Wiley-Blackwell Publishing Ltd, Mar 2017.
The definitive version is available at https://doi.org/10.1002/2016WR019861

AGU PUBLICATIONS

Water Resources Research

RESEARCH ARTICLE
10.1002/2016WR019861

Key Points:
- Groundwater withdrawal during the 2007–2010 drought in the San Joaquin Valley, California caused significant subsidence
- Geomechanical properties, geologic data, and water level data were integrated with InSAR to estimate inelastic deformation
- Results indicate that the majority of deformation that occurred over this time period was inelastic

Supporting Information:
- Supporting Information S1

Correspondence to:
R. Smith,
rgsmith@stanford.edu

Citation:
Smith, R. G., R. Knight, J. Chen, J. A. Reeves, H. A. Zebker, T. Farr, and Z. Liu (2017), Estimating the permanent loss of groundwater storage in the southern San Joaquin Valley, California, *Water Resour. Res.*, *53*, 2133–2148, doi:10.1002/2016WR019861.

Received 30 SEP 2016
Accepted 19 FEB 2017
Published online 13 MAR 2017

Estimating the permanent loss of groundwater storage in the southern San Joaquin Valley, California

R. G. Smith[1], R. Knight[1], J. Chen[1], J. A. Reeves[1], H. A. Zebker[1], T. Farr[2], and Z. Liu[2]

[1]Department of Geophysics, Stanford University, Stanford, California, USA, [2]Jet Propulsion Laboratory, California Institute of Technology, Pasadena, California, USA

Abstract In the San Joaquin Valley, California, recent droughts starting in 2007 have increased the pumping of groundwater, leading to widespread subsidence. In the southern portion of the San Joaquin Valley, vertical subsidence as high as 85 cm has been observed between June 2007 and December 2010 using Interferometric Synthetic Aperture Radar (InSAR). This study seeks to map regions where inelastic (not recoverable) deformation occurred during the study period, resulting in permanent compaction and loss of groundwater storage. We estimated the amount of permanent compaction by incorporating multiple data sets: the total deformation derived from InSAR, estimated skeletal-specific storage and hydraulic parameters, geologic information, and measured water levels during our study period. We used two approaches, one that we consider to provide an estimate of the lowest possible amount of inelastic deformation, and one that provides a more reasonable estimate. These two approaches resulted in a spatial distribution of values for the percentage of the total deformation that was inelastic, with the former estimating a spatially averaged value of 54%, and the latter a spatially averaged value of 98%. The former corresponds to the permanent loss of 4.14×10^8 m^3 of groundwater storage, or roughly 5% of the volume of groundwater used over the study time period; the latter corresponds to the loss of 7.48×10^8 m^3 of groundwater storage, or roughly 9% of the volume of groundwater used. This study demonstrates that a data-driven approach can be used effectively to estimate the permanent loss of groundwater storage.

Plain Language Summary Subsidence due to groundwater pumping from 2007 to 2010 in the San Joaquin Valley, California was mapped using satellite data known as InSAR. These data were incorporated with additional datasets, including geological information, to estimate how much subsidence was permanent. This subsidence represents a permanent loss in groundwater storage. Using these methods, we estimated that a permanent loss of 7.48×10^8 m^3 of groundwater storage occurred during our study period. This accounted for roughly 9% of groundwater pumping in our study area. While this is just a small fraction of the total water stored underground in this area, this 'water of compaction' is an important safeguard for times of drought that, once removed, cannot be replenished.

1. Introduction

California's Central Valley is a highly productive agricultural region in the United States. Due to its water-intensive crops and arid climate, it accounts for roughly one fifth of the nation's groundwater usage [*Faunt et al.*, 2009b]. The recent droughts in California have further increased the groundwater demand, causing groundwater depletion throughout the valley. One concerning consequence of groundwater depletion in the Central Valley is wide-scale subsidence due to compaction of the sediments in the aquifer system. The compaction and subsidence has been most pronounced in the San Joaquin Valley, which is located in the southern two thirds of the Central Valley. In particular, the southern half of the San Joaquin Valley has experienced the most subsidence.

The compaction rate in the southern San Joaquin Valley was as much as 30 cm/yr from the 1920s to 1970s, but was largely arrested when the state developed surface water routing systems to decrease reliance on groundwater [*Poland et al.*, 1975]. Over the past decade, however, reliance on groundwater has increased due to droughts and the increased planting of water-intensive crops. Ground subsidence in the San Joaquin Valley has numerous negative effects, including damaging buildings, well casings, bridges,

water conveyance structures, permanently removing groundwater storage, and decreasing pore space and permeability within the aquifer [*Galloway and Riley*, 1999; *Faunt et al*., 2009b].

One major question raised by water managers and policy-makers, related to the ongoing subsidence in the San Joaquin Valley, is whether the subsidence is permanent (inelastic deformation), representing a nonrecoverable loss of groundwater storage, or whether the level of the ground surface and water storage capacity of the aquifers and aquitards will recover. This question is typically addressed using a three-dimensional (3-D) groundwater model, which solves for the head at each element of the model over time and space [*Helm*, 1975; *Leake*, 1990; *Hoffmann et al*., 2003a]. Many of the commonly used groundwater modeling codes have built in subsidence modules that can model compaction of aquifers and aquitards [*Hoffman et al*., 2003b; *California Department of Water Resources*, 2007]. However, building and calibrating a 3-D groundwater model is very time-consuming and expensive. In addition, to accurately determine the amount of inelastic deformation, the model requires as an input the lowest head previously experienced by the aquifer or aquitard (referred to as the preconsolidation head). This value is very difficult to estimate, especially in the Central Valley where water level data reporting has many temporal gaps. Furthermore, to be useful in addressing ongoing questions such as subsidence, a groundwater model must be updated regularly, which further adds to the cost and time demand. Studies such as *Bell et al*. [2008] and *Chaussard et al*. [2014] compared multidecade InSAR time series with head levels to estimate long-term trends in deformation as a response to changes in head. *Bell et al*. [2008] estimated inelastic deformation using InSAR by assuming inelastic deformation was the long-term signal of ground deformation. However, over short time scales such as the 2007–2010 California drought examined in this study, without knowledge of the preconsolidation head it is unknown whether the ground will rebound once water levels rise to their predrought levels.

Faunt et al. [2016] estimated that most of the recent subsidence in the Central Valley was due to inelastic deformation. Their study used water level data from the California Department of Water Resources to determine what fraction of wells dropped below their historically lowest water level (preconsolidation head) during the recent 2007–2010 and 2012–2015 droughts. When water levels drop below their preconsolidation head, the aquifer system reaches new levels of effective stress and inelastically deforms [*Terzaghi*, 1925; *Poland,* 1975]. The study of *Faunt et al*. [2016] estimated that most wells in the San Joaquin Valley did drop below their preconsolidation head during the recent droughts. Their study provided useful qualitative information about the nature of subsidence in the Central Valley. The publications by *Faunt et al*. [2016] and *Farr and Liu* [2015] both estimated the amount of subsidence over parts of the San Joaquin Valley using InSAR. The goal of this study is to further develop the ability of InSAR to be used to spatially map changes in groundwater storage.

In this study we present a method that can be used to quantitatively estimate how much compaction is permanent, and how it varies spatially. The time frame of our study is from 2007 to 2010, during which time the Central Valley experienced a significant drought that increased farmers' reliance on groundwater and in turn resulted in wide-spread land subsidence. We used recent water level data along with InSAR-derived subsidence for the time period June 2007 to December 2010, and previously estimated geomechanical properties of sediments in the area to obtain an estimate of permanent compaction and loss of groundwater storage in the southern portion of the San Joaquin Valley. This method does not require knowledge of the preconsolidation head, nor does it require the calibration of a groundwater model, allowing it to be effectively implemented in areas that have limited data.

2. Background

2.1. The Link Between InSAR Data and Hydraulic Head

Synthetic Aperture Radar (SAR) is a microwave imaging system, which uses a radar antenna mounted on an airborne or satellite-based platform to transmit and receive electromagnetic (EM) waves [*Madsen and Zebker*, 1998; *Rosen et al*., 2000]. The difference in the phase of the EM wave as measured between two acquisitions can be related to the change in elevation of Earth's surface that has occurred. The process of using multiple SAR images interferometrically in this manner is referred to as Interferometric Synthetic Aperture Radar, or InSAR.

In the application of InSAR to studies of groundwater systems, it is assumed that the change in elevation obtained from the InSAR measurement is due to the change in the total integrated thickness of the

underlying material (aquifers and aquitards) due to the withdrawal and recharge of groundwater; the former causing a decrease in elevation and the latter an increase. Here we use "aquifer" to denote the coarse, more permeable material; "aquitard" or "clay layer" to denote fine-grained, less permeable material; and "aquifer system" to denote the heterogeneous combination of both aquifers and aquitards. The following equations outline the relationship between changes in water level (head) and changes in aquifer system thickness.

The link between changes in aquifer system thickness and changes in hydraulic head is based on the relationship between pore pressure and effective stress, developed by *Terzhaghi* [1925]

$$\sigma_e = \sigma_T - P_p, \tag{1}$$

where σ_e is the effective stress, σ_T is the total stress related to the weight of the overburden, and P_p is the pore pressure. In confined aquifer systems, we assume a constant overburden stress, as the saturated thickness does not change with a change in head, so differentiating equation (1) yields

$$\Delta\sigma_e = -\Delta P_p. \tag{2}$$

Further, in a confined aquifer system $\Delta P_p = \Delta h \rho_w g$, where Δh is the change in hydraulic head, ρ_w is the density of the water, and g is gravitational acceleration, so $\Delta\sigma_e = -\Delta h \rho_w g$. *Jacob* [1940] used this principle to define the specific storage, or S_s, as the volume of water produced per unit volume of the aquifer system per unit change in head, while remaining saturated. S_s is given by the following equation:

$$S_s = \rho_w g(\alpha + \eta\beta), \tag{3}$$

where α is the compressibility of the sediment, η is the porosity, and β is the compressibility of water. Equation (3) can be separated into two components

$$S_s = S_{sk} + S_{sw}, \tag{4}$$

where $S_{sk} = \rho_w g \alpha$ is the skeletal-specific storage, which relates the deformation of the aquifer system to the change in effective stress, and can be rewritten as

$$S_{sk} = \frac{\Delta b}{b_0 \Delta h}, \tag{5}$$

where Δb is the change in thickness of the compacting material; Δh is the change in head experienced by the compacting material; and b_0 is the original thickness of the material that is experiencing a change in head, also referred to as the saturated thickness. This value is time-dependent and related to the degree to which the compacting material equilibrates with a change in head in the aquifer system. This is a function of the hydraulic conductivity and specific storage of the sediment; for example, a thick clay aquitard may only experience a significant change in head (over a short time period) near its border with an aquifer, due to delayed drainage caused by low hydraulic conductivity. Thus, its b_0 value over a short time period would be lower than its total thickness. The other component of equation (4) is $S_{sw} = \rho_w g n \beta$, which relates the deformation of water to the change in effective stress. Using typical values for ρ_w and g, 4.6×10^{-10} m^2/N for β as reported by *Fetter* [2001], and assuming a porosity, η, of 0.3, S_{sw} is estimated to be 1.35×10^{-6} m^{-1}.

In unconfined aquifers, compaction and expansion can also occur, but the overburden stress is not constant because the aquifer thickness changes with a change in head. Because of this, the effective stress is a function of the change in head as well as the amount of water that drains from or recharges the aquifer per unit head. This is shown in the following equation:

$$\Delta\sigma_e = -\left(1 - S_y\right)\Delta P_p, \tag{6}$$

where S_y is the specific yield [*Leake and Galloway*, 2007; *Poland and Davis*, 1969]. S_y has been estimated to be 0.1 in the San Joaquin Valley [*Williamson et al.*, 1989]. Thus, the change in effective stress in an unconfined aquifer, and by extension the amount of compaction experienced in an unconfined aquifer, could be approximated in the same way as with a confined aquifer, then multiplied by $\left(1 - S_y\right) = 0.9$.

Deformation in response to a decrease in head (increase in σ_e) can be elastic, so the loss of thickness can be recovered with an increase in head, or inelastic, where the compaction is permanent; permanent

compaction in unconsolidated sediments is caused by rearrangement of the grains at the pore scale. Unconsolidated sand does not typically deform inelastically in the pressure conditions existing in aquifers. However, clays in aquifers can deform inelastically given certain stress conditions. Following the work of *Poland et al*. [1975], we assume that deformation is elastic unless σ_e is greater than the historic maximum value σ_{emax}. The head corresponding to σ_{emax} is referred to as the preconsolidation head, so if the head drops below the preconsolidation head, inelastic deformation will occur and the compaction is permanent. The convention is to add "−e" to the subscript for skeletal-specific storage to denote elastic deformation (S_{ske}) and "−v" to denote inelastic deformation (S_{skv}).

Equation (5) can be separated into its inelastic and elastic components

$$S_{sk} = S_{skv} + S_{ske}, \tag{7}$$

where S_{skv} is the inelastic skeletal-specific storage. It is given by the equation below

$$S_{skv} = \frac{\Delta b_{inelastic}}{b_{0v}\Delta h_{inelastic}}, \tag{8}$$

where $\Delta h_{inelastic}$ is the drop in head below the preconsolidation head, $\Delta b_{inelastic}$ is the inelastic portion of deformation, and b_{0v} is the thickness of sediment that experienced inelastic deformation. Referring back to equation (7), S_{ske} is the elastic skeletal-specific storage, and is given by

$$S_{ske} = \frac{\Delta b_{elastic}}{b_{0e}\Delta h_{elastic}}, \tag{9}$$

where $\Delta h_{elastic}$ is the drop in head that remains above the preconsolidation head, $\Delta b_{elastic}$ is the elastic portion of deformation, and b_{0e} is the thickness of sediment that experienced elastic deformation.

There are significant differences in the magnitude of S_{sk} for unconsolidated materials undergoing elastic and inelastic deformation. Most studies estimate that S_{skv} is 10–100 times larger than S_{ske} [*Sneed*, 2001; *Faunt et al*., 2009b; *Riley*, 1998].

In addition to these differences in the mechanical properties of materials impacting the magnitude of deformation in aquifer systems, differences in hydrologic properties determine the timing of the deformation relative to the timing of groundwater withdrawal or recharge. While the sands in an aquifer system typically equilibrate quickly with changes in head at the wellbore (and thus deform quickly), clays often have a time lag. This timing is governed by the one-dimensional (vertical) diffusion equation [*Helm*, 1975], shown here

$$\frac{\partial}{\partial z}\left(K_v \frac{\partial h}{\partial z}\right) = S_s \frac{\partial h}{\partial t}, \tag{10}$$

where K_v is the vertical hydraulic conductivity, S_s is the specific storage, h is the hydraulic head, z is depth, and t is time. Assuming K_v is uniform with depth, it can be placed outside of the partial derivative. Under this condition, the time it takes for a given hydrologic unit to equilibrate with the hydrologic head above and below it, denoted as τ, can be approximated by the following equation when there is a step decrease in hydraulic head of equal magnitude on both boundaries of the unit [*Scott*, 1963; *Riley*, 1969]:

$$\tau \simeq \left(\frac{b_0}{2}\right)^2 S_s/K_v, \tag{11}$$

where b_0 is the thickness of the equilibrated hydrologic unit. *Sneed* [2001] compiled a list of estimates of K_v, S_{ske}, and S_{skv} of clay layers, which were estimated by modeling the diffusion and compaction of clay layers at sites in the San Joaquin Valley where detailed information on pressure history and clay thickness were available. Estimates of K_v range from 1.67×10^{-8} to 2.48×10^{-6} m/d with an average of 1.23×10^{-6} m/d. The average of estimates for S_{skv} is 9.3×10^{-4} m^{-1}, and values range from 4.6×10^{-4} to 2.2×10^{-3} m^{-1}. The average S_{ske} is 1.5×10^{-5} m^{-1}, and ranges from 6.6×10^{-6} to 2.5×10^{-5} m^{-1}. *Sneed* [2001] also compiled property estimates for sands in the San Joaquin Valley: the average S_{ske} is 5.6×10^{-6} m^{-1} and ranges from 1.4×10^{-6} to 1.6×10^{-5} m^{-1}. Estimates of S_{ske} in aquifer systems in the San Joaquin Valley that are composed of aggregate combinations of sand and clay range from 2.0×10^{-6} to 2.3×10^{-5} m^{-1} with an average of 9.0×10^{-6} m^{-1}.

The vertical diffusivity, referred to throughout the paper as simply the diffusivity D, is defined as K_v/S_s, so equation (11) can alternatively be written as

$$\tau \simeq \frac{\left(\frac{b_0}{2}\right)^2}{D}. \tag{12}$$

Thus for clay layers, the delayed drainage time, τ, is proportional to the square of the half thickness, $\left(\frac{b_0}{2}\right)^2$, and inversely proportional to diffusivity, D. Equation (12) can be rearranged to solve for b_0, giving

$$b_0 \cong 2\sqrt{\tau D}. \tag{13}$$

Since S_s is very different under elastic conditions than inelastic conditions, D varies significantly based on whether the sediment that is compacting is deforming elastically or inelastically. Combining the range of values of K_v and adding S_{sw} to the range of values of S_{skv} and S_{ske} reported by *Sneed* [2001], D ranges from 6.43×10^{-4} m^2/d to 3.59×10^{-1} m^2/d with an average of 7.60×10^{-2} m^2/d during elastic deformation of clays. During elastic deformation of mixed sand and clay systems, it ranges from 6.87×10^{-4} m^2/d to 8.55×10^{-1} m^2/d with an average of 1.19×10^{-1} m^2/d. During inelastic deformation of clays, it ranges from 7.59×10^{-6} m^2/d to 6.16×10^{-3} m^2/d with an average of 1.32×10^{-3} m^2/d.

2.2. The Hydrogeology of the Study Area

Our study area is in the southern portion of the San Joaquin Valley and includes four different subbasins: Kings, Kaweah, Tulare Lake, and Tule. These subbasins, as well as our study area, are shown in Figure 1. We chose this as our study area because of the large historic subsidence bowl and recent subsidence in the center of the study area. We limited the study area to where we had well coverage. The subsurface of our study area is a mix of sand, gravel, and clay layers of variable thickness. The upper 400–800 m, generally considered as the aquifer system, are continental sediments, derived from the Sierra Nevada and Coast Ranges. Below this are less permeable continental sediments with saline pore water and a thick (approximately 6 km) package of marine sediments with low hydraulic conductivities, assumed to be a no-flow boundary by previous groundwater studies in the San Joaquin Valley [*Williamson et al.*, 1989]. In the western half of our study area, the Corcoran clay, which ranges in thickness from 0 to 20 m, separates the upper and

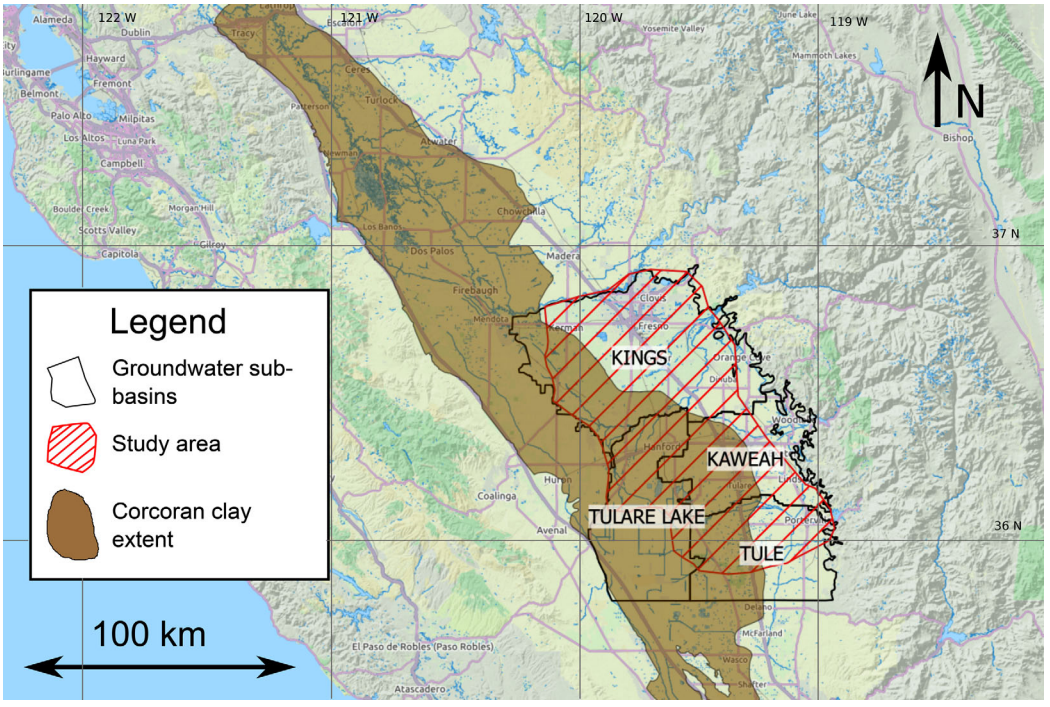

Figure 1. Map of our study area, shown in red. The study area was limited by areas that had water level measurements. The approximate extent of the Corcoran clay, as mapped by *Page* [1986] is shown in brown. The four subbasins that overlap with our study area are also shown: Kings, Kaweah, Tulare Lake, and Tule.

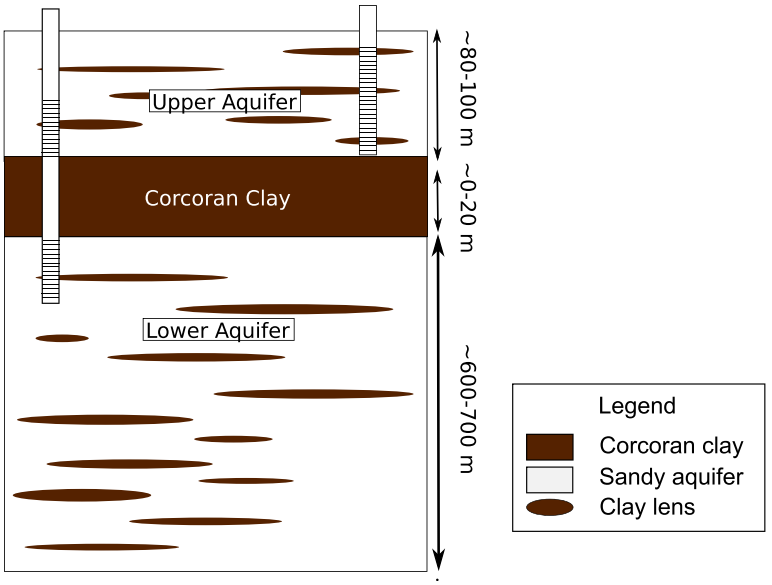

Figure 2. Simplified geologic cross section of our study area.

lower aquifers. The extent of the Corcoran clay, determined by *Page* [1986] using a combination of electric logs and lithology logs, is shown in Figure 1. Figure 2 shows a generalized, simplified cross section of the upper 800 m of the subsurface of our study area, which includes an upper aquifer, the Corcoran clay, and a lower aquifer. Note that in both the upper and lower aquifers, numerous thin clay layers exist. These thin clay layers can act as small-scale confining units, creating semiconfined conditions above the Corcoran clay.

Deformation in the southern San Joaquin Valley could potentially come from multiple sources. Although the Corcoran clay is the main confining unit in the area, other, less extensive clay units of varying thickness throughout the upper and lower aquifers can also deform. The upper and lower aquifers as well as the Corcoran clay can deform elastically when the pre-consolidation head has not been reached.

3. Method for Estimating Permanent Loss of Storage

To estimate the permanent loss of storage over the time period 2007–2010, we used a system of constitutive geomechanical equations. We defined the total deformation (Δb_{tot}) as the sum of its inelastic and elastic components, and the total change in head (Δh_{tot}) as the difference between the highest head and the lowest head experienced during our study period. Since virtually all wells experienced a head decline, this number is negative. We divide Δh_{tot} into the sum of its drop in head while above the preconsolidation level (i.e., in the elastic deformation range), during the study time period, $\Delta h_{elastic}$, and its drop in head while below the preconsolidation level (i.e., in the inelastic deformation range) $\Delta h_{inelastic}$. This assumes that the elastic contribution to deformation is negligible when inelastic deformation is occurring

$$\Delta b_{tot} = \Delta b_{inelastic} + \Delta b_{elastic}, \tag{14}$$

$$\Delta h_{tot} = \Delta h_{inelastic} + \Delta h_{elastic}. \tag{15}$$

We used equations (8) and (9), rearranging them in the following way

$$\Delta h_{inelastic} = \frac{\Delta b_{inelastic}}{b_{0v} S_{skv}}, \tag{16}$$

$$\Delta h_{elastic} = \frac{\Delta b_{elastic}}{b_{0e} S_{ske}}. \tag{17}$$

This system of four equations contains ten variables. We were able to estimate six of these variables from measurements: Δb_{tot}, Δh_{tot}, S_{skv}, S_{ske}, b_{0v}, and b_{0e}. The variable Δb_{tot} was measured using InSAR. The

parameter Δh_{tot} was estimated by determining the maximum drop in head between 2007 and 2010. We obtained a range of estimates for S_{skv} and S_{ske} from *Sneed* [2001]. The saturated thicknesses, b_{0v}, and b_{0e}, are the initial thicknesses of the compacting sediment when deforming inelastically or elastically, respectively. Hereafter we use the term b_0 only in cases that apply to both b_{0v} and b_{0e}. Since compaction is dominated by clays in inelastic deformation [*Sneed*, 2001], we assumed that b_{0v} represents the thickness of compacting clays. For the case of elastic deformation (b_{0e}), we calculated the compacting sediment using estimates of the sand and clay thickness. The total thickness of coarse- and fine-grained deposits of the aquifer system has been estimated by *Faunt et al*. [2009a], so we used that as a basis for estimating b_{0e}. For the case of inelastic deformation (b_{0v}), we only used the clay thickness for our calculation of the compacting sediment. In order to calculate the thickness of compacting clay from the total clay thickness, we needed estimates of diffusivity (D) and the thickness of the clay layers. We calculated what we assumed to be the maximum possible b_0 values by assuming a sufficiently high D and/or low thickness of clay beds that all clay beds equilibrated and compacted between 2007 and 2010. We made lower, more reasonable estimates of b_0 by setting D equal to the average reported values under inelastic deformation ($D = 1.4 \times 10^{-3}$ m^2/d) and calculating the amount of clay that would compact over our study period under those conditions.

This left us with four equations and four unknowns: $\Delta b_{inelastic}$, $\Delta b_{elastic}$, $\Delta h_{inelastic}$, and $\Delta h_{elastic}$. The purpose of our study was to calculate the portion of the deformation that is permanent compaction so we solved for $\Delta b_{inelastic}$, obtaining

$$\Delta b_{inelastic} = -\frac{S_{skv} b_{0v} (\Delta h_{tot} S_{ske} b_{0e} - \Delta b_{tot})}{S_{skv} b_{0v} - S_{ske} b_{0e}}. \quad (18)$$

In the following sections we describe the approach taken to estimate the parameters needed to solve equation (18).

3.1. Estimating Δb_{tot} Using InSAR

The InSAR processing technique for this data set has been previously published in *Farr and Liu* [2015] but we will briefly summarize the processing methodology here. L-band ALOS PALSAR scenes were acquired over the San Joaquin Valley from the Alaska Satellite Facility (https://www.asf.alaska.edu/). Seventeen acquisitions of the ascending track 218 between 21 June 2007 and 30 December 2010 were processed using a modified version of JPL/Caltech ROI-PAC software package. Forty-three interferograms were formed based on the spatial and temporal baseline thresholds (less than 800 m and 4 years) and the topographic phase was removed using the SRTM 3 arc sec digital elevation database. To improve the phase coherence, power-spectrum (PS) filtering was applied to each individual interferogram and the interferograms were multilooked in range and azimuth by 32 and 64 pixels, respectively, producing roughly 250 $\times$ 250 m pixels. The interferograms were unwrapped using SNAPHU and minimum-cost flow algorithm [*Chen and Zebker*, 2001]. A long-wavelength ramp in each interferogram due to orbital errors and northwestward tectonic motion was also removed.

In order to solve for the long-term line-of-sight (LOS) deformation velocity from these unwrapped interferograms, a variant of Small Baseline Subset (SBAS) InSAR time series inversion analysis was used, with a linear deformation model [e.g., *Berardino et al*., 2002; *Sansosti et al*., 2010]. Residual DEM error correction was incorporated in the time series analysis. Spatiotemporal filtering was used to remove high-frequency turbulent troposphere noise [*Berardino et al*., 2002; *Samsonov*, 2010; *Farr and Liu*, 2015]. To ensure that only highly coherent pixels were used in the time series analysis, analysis was limited to the pixels that had coherence ($>$0.5) in at least 60% of the filtered interferograms. As InSAR measures relative LOS motion referenced to a given location, InSAR deformation measurements were calibrated to the Plate Boundary Observation (PBO) network GPS station P725 (http://www.unavco.org/instrumentation/networks/status/pbo/overview/P725) about 30 km north of Fresno near Coarsegold, CA, where no significant vertical deformation occurred during the study period. The vertical displacement of this GPS station is shown in Figure S1 of Supporting Information. From these methods, the total displacement along the LOS was determined.

For the purposes of this study, we calculated the InSAR LOS look angle and converted the InSAR LOS deformation to vertical subsidence, or Δb_{tot}. This assumes that there was negligible spatial variation in horizontal displacement during our study period which is considered to be valid based on the existing GPS data over the study area. Figure 3 shows the total vertical subsidence for the period of June 2007 to December 2010.

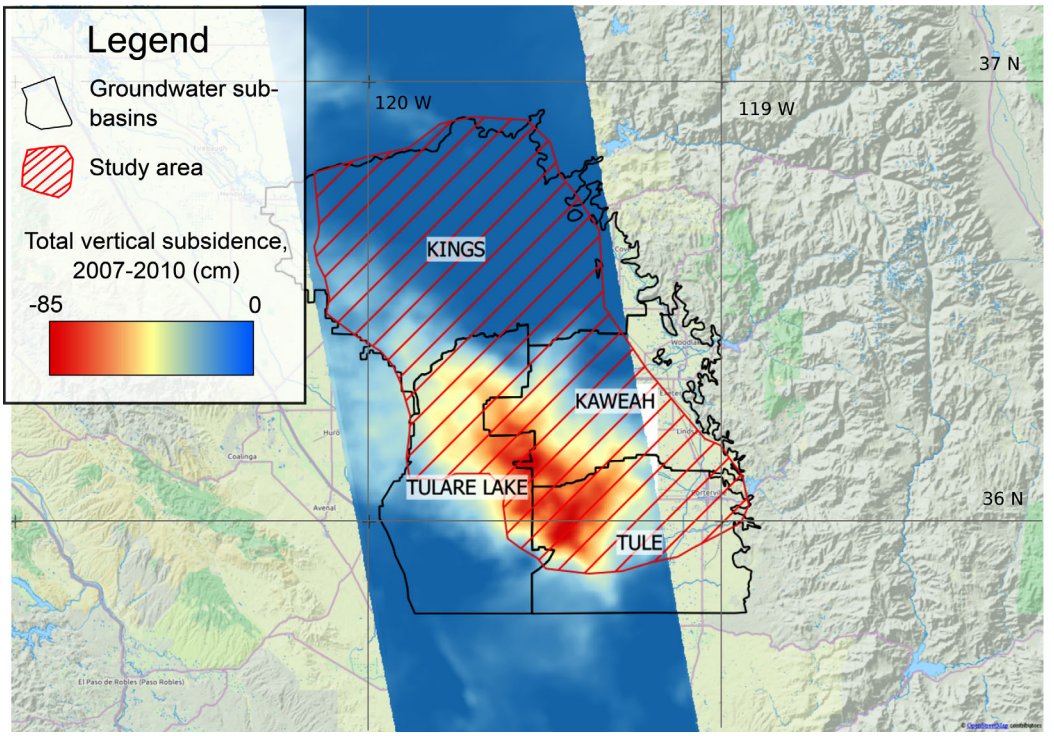

Figure 3. Map of InSAR-derived total vertical subsidence from June 2007 to December 2010 (modified from *Farr and Liu* [2015]).

As a further check on the validity of our maps and time series, we compared our results to other GPS stations (for example, P307 shown in Figure S2 of the Supporting Information). The result shows good agreement in the long-term trends with small short-term departures, most likely caused by decorrelation noise or residual tropospheric water vapor variations, both of which can impact the InSAR deformation estimate. Another validation of the time series and subsidence interpretations would be comparison to extensometer measurements. Unfortunately, no extensometers were active in the area during the period of our study.

3.2. Estimating Δh_{tot}

In order to estimate how much compaction was permanent, we needed to know the change in head in the time period 2007–2010. This requires water level data which are available throughout our study area with fairly good spatial density. There are 945 wells in our area containing data over the study period. The data are provided through the Water Data Library of the California Department of Water Resources (http://www.water.ca.gov/waterdatalibrary/). Some of these wells (∼10%) contain a water level record going back to the 1960s and earlier.

We initially assumed that we would need to determine head levels in the upper aquifer and lower aquifer, as both could contribute to compaction. However, we found from comparing head levels in the lower aquifer with head levels in the upper aquifer, that the two aquifers have similar head levels, closely track each other over time and have seasonal head changes of similar magnitude, indicating that the aquifers are fairly well connected. This is likely caused by several factors—widespread wellbore leakage [*Williamson et al.*, 1989; *Faunt et al.*, 2009b] and a relatively thin Corcoran clay over most of the study area. It has been suggested that the presence of numerous clay layers above the Corcoran clay create semiconfined conditions [*Williamson et al.*, 1989]. For these reasons, we treated the whole aquifer system as one semiconfined to confined unit. This approach is similar to that of *Williamson et al.* [1989]. We used estimates from *Faunt et al.* [2009a] for the depth of the aquifer system, which ranges from 470 to 760 m.

Figure 4 illustrates how the difference between the maximum and minimum head (Δh_{tot}) experienced from June 2007 to December 2010 was calculated. This figure has average water levels taken from ∼80 wells in our study area. Note that the average pattern in head levels shows a sharp decrease in head in 2008, and

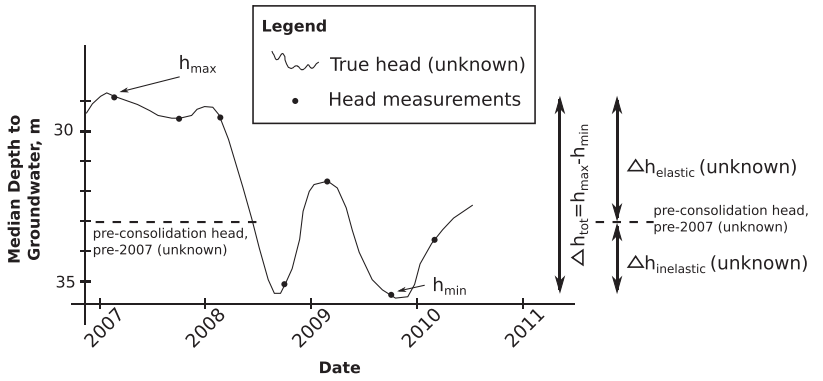

Figure 4. Illustration of how Δh_{tot} was calculated. The dashed line represents the unknown preconsolidation head, which separates $\Delta h_{elastic}$ from $\Delta h_{inelastic}$. The measurements of head drop shown are averaged from ~80 wells in our study area. Note that the infrequent sampling causes some loss of information in calculating Δh_{tot}. Note that the head remained below its 2007–2008 levels for at least 2 years. The dashed preconsolidation head line is unknown, and its position is merely hypothetical. Also note that while depth to groundwater is shown in this figure, head as meters above mean sea level is used in the actual calculations.

water levels remain low for approximately 2 years. Also note the relatively low sampling frequency. Most of the wells that we used were sampled, during this time period, once in the late winter/early spring (typically between January and March) when water levels are at or near their highest point, and once in the fall (typically between September and November) when water levels are at or near their lowest point. While a greater density of temporal sampling would be ideal, we assumed that the difference between the highest level measured in the spring samplings and the lowest level measured in the fall samplings provides a good estimate of the maximum head drop, Δh_{tot} experienced at a well location, especially during periods of drought when long-term trends dominate over seasonal head variations. One advantage to our method is that even though the preconsolidation head is unknown, we can still calculate the amount of inelastic deformation. Typical methods that require knowledge of the preconsolidation head would introduce significant error in our study area since historic head levels have a high degree of uncertainty.

By only considering the head change between 2007 and 2010 to compare with the deformation observed by InSAR from 2007 to 2010, we assumed that all deformation that occurred between 2007 and 2010 was related to the change in head from 2007 to 2010. We did this because significant delayed deformation signals related to changes in head prior to 2007 were not observed in continuous GPS data in the area (see Figure S3 of Supporting Information). Since there were no major droughts 2 years prior to our study period, we considered the assumption that all deformation occurring between 2007 and 2010 was related to changes in head within the same time window to be valid.

For the purposes of our study, we needed to have head measurements that were representative of the regional head levels. Most of the head measurements used in our study come from irrigation wells, which are regularly pumped for groundwater. If head is measured shortly after the pump is turned off, the measurement will be affected by the cone of depression and not be representative of regional head levels. A head measurement at one well can also be impacted by pumping at near-by wells. The approach we took was to find locations where we had at least three wells within a radius of 5 km, and to average all of the head measurements within that window using a spatial moving average filter to suppress the effects due to cone-of-depression.

3.3. Estimating b_0

The value of b_0 is the total thickness of sediment that experienced compaction during the 42 months of our study period. We assumed that during our study period, sand layers within the aquifer system (as defined in 3.3.1 and 3.3.2) completely equilibrated with the change in head experienced at the wellbore and compacted. Referring to the thickness of clay that experienced compaction, we defined it as

$$b_0 = \sum_{i=1}^{N} b_{0i}, \tag{19}$$

where N is the total number of clay layers and b_{0i} is the portion of a single layer that was subject to compaction in that time period. As discussed in the background section, the portion of a clay layer that drains and experiences compaction can be approximated with knowledge of the time given to drain (τ) and the

diffusivity (D), given by equation (13). An individual clay layer, b_{0i}, has finite thickness; the thickness that compacts cannot exceed the total thickness of that layer. Thus, b_{0i} is given by

$$b_{0i} = \min\left(2\sqrt{\tau D_i},\ b_{Ti}\right), \tag{20}$$

where b_{Ti} is the total thickness of the given layer, and D_i is the diffusivity of the layer. To accurately estimate these would require a detailed geologic model showing the location and thickness of each clay layer, the locations of all perforated intervals in wells, and knowledge of the diffusivity of all materials in the aquifer system. We chose to take two approaches to determining the values of b_0, first estimating what we assume to be their maximum values, and then refining that estimate to a lower, more reasonable estimate using other available information.

3.3.1. Upper b_0 Estimate

The best information about the amount and distribution of clay is available in the study by *Faunt et al*. [2009a] who classified cuttings from over 8000 driller's logs as either fine-grained or coarse-grained, and determined the percentage of each over 15 m depth intervals. They then interpolated these data over the Central Valley using a geostatistical method known as kriging. The grid spacing for the resulting geologic model is 1 mile, and the size of the depth intervals is 15 m. From this, the thickness of clay in each 15 m interval can be determined by multiplying the fraction of fine-grained material by 15 m. The geologic model also provides the depth to the base of the aquifer. We summed the clay thickness over all 15 m intervals above the base of the aquifer system, which ranged in depth from 470 to 760 m to determine the total clay thickness of the aquifer system, b_T.

We used this information to obtain an estimate of b_{0v} at each land surface location (grid cell) in the model of *Faunt et al*. [2009a]. To estimate b_{0e}, we summed the thickness of all sands and clays from the geologic model. Our simple conceptual model was the following: At each surface location, all of the material in the aquifer system, from the top of the perforated interval to the base of the aquifer system, equilibrated with the head change that occurred due to pumping at any depth at that surface location. This assumes that the diffusivity of the clay layers is sufficiently high and/or the thicknesses of the clay layers are sufficiently small that all available clay below the top of the perforated interval equilibrated with the head change and compacted. It also assumes that the diffusivity of the aquifer-system as a whole is sufficiently high that the deep portions of the aquifer equilibrated quickly with the head changes experienced in the wellbore, which is typically much shallower. We used these simplifying assumptions to make an estimate of what we consider to be the maximum possible clay thickness that could compact. For each clay layer i, $b_{Ti} < 2\sqrt{\tau D}$, so that $b_{0i} = b_{Ti}$ and thus $b_0 = \sum_{i=1}^{n} b_{Ti} = b_T$. The resulting maximum possible value for b_{0v} is therefore the total thickness of clay in the aquifer system as represented in the geologic model by *Faunt et al*. [2009a]. This ranges from 197 to 514 m in the southwest of our study area; this result is shown in Figure 6a. The resulting values for b_{0e} range from 263 to 655 m, and are shown in Figure S4 of Supporting Information.

3.3.2. Lower b_0 Estimate

Our other approach involved estimating b_0 by summing b_{0i} using equation (20). This method calculated the estimated thickness of clay that compacted during our study period. To accurately do this required a reasonable estimate of diffusivity, D and the drainage time, τ. A reasonable estimate of the drainage time would be the duration of time that water levels were at or near their lowest point. This is the time during which compaction in the clays can occur—once water levels rise again, drainage from the clays into the aquifer system stops. A longer duration would mean any given clay layer would have more time to equilibrate with the drop in head experienced by the aquifer, and compact more. Our study period covered 3.5 years, but based on average head levels (Figure 4) and modeled change in groundwater storage [*Faunt et al*., 2016], it appears that on average the head levels were at or near their lowest point for only about 2 years of our study period. For this reason we chose 2 years for the delay time, τ. Note that τ as described here is not describing the time it will take for the entire aquifer system to equilibrate with a drop in head, but rather the duration of our study period where water levels were at or near their lowest level. This was done so that we could estimate the fraction of clay that compacted during our study period, rather than the total clay of the aquifer system.

As a limiting assumption that significant diffusion outside of the estimated upper and lower perforated intervals in wells did not occur, we summed clay layers between these intervals. Since perforated intervals of irrigation wells are typically not reported, we used an estimate of perforated intervals from the

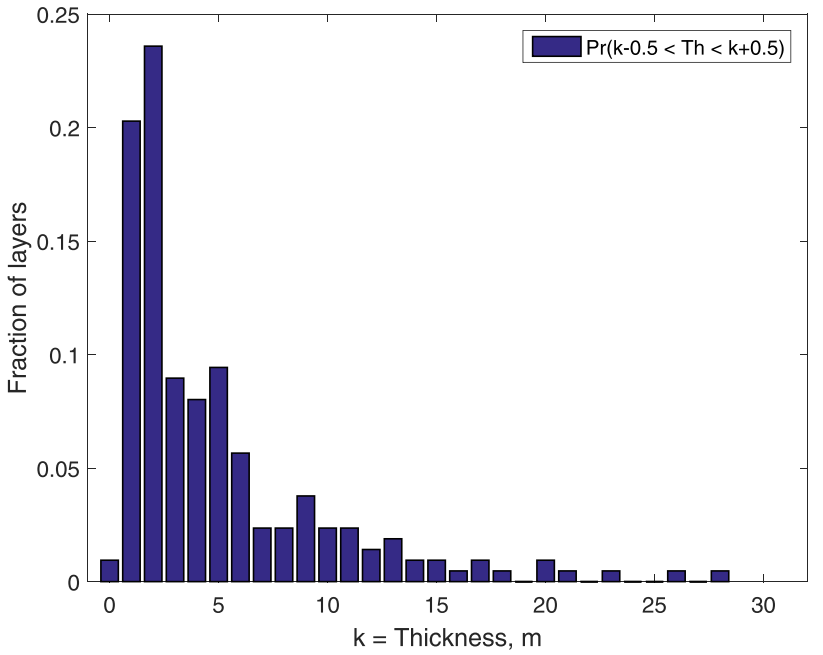

Figure 5. Number of layers in a given thickness bin (*k*) divided by the total number of layers, with thicknesses binned in 1 m intervals from 0 to 30 m.

groundwater model of *Faunt et al*. [2009b]. This model has the same grid spacing (1 mile between cells) as the geologic model of *Faunt et al*. [2009a].

To calculate b_{0v}, we chose to use the average diffusivity under inelastic conditions as determined from the range reported by *Sneed* [2001]: 1.32×10^{-3} m^2/d. To calculate b_{0e}, we used the average diffusivity under elastic conditions of clays from the values reported by *Sneed* [2001]: 7.60×10^{-2} m^2/d. Using these values for D and τ, we determined $2\sqrt{\tau D}$ to be 2.0 m for the inelastic case and 19 m for the elastic case. Thus, taking for example the inelastic case, if $b_{Ti} < 2.0\ m$, then $b_{0i} = b_{Ti}$ but if $b_{Ti} > 2.0\ m$, then $b_{0i} = 2.0\ m$. Solving for b_0 thus required knowledge of the number and thickness of all clay layers in the perforated interval.

While the model of *Faunt et al*. [2009a] provides estimates of total clay thickness within depth intervals, it does not provide information about the number or thickness of individual clay layers. We chose to estimate the probability that a clay layer in the subsurface would have a given thickness, *k*, by recording the thickness of all clay layers reported in 12 drillers' logs in our study area. From this we obtained a distribution of clay layer thicknesses (see Figure 5), with a maximum thickness of approximately 30 m. We assumed that the probability of a clay layer having a given thickness was stationary throughout our study area. With this information, we were able to estimate b_0 as follows:

$$b_0 = N \sum_{k=0}^{30} \Pr\left(k-0.5 < Th \le k+0.5\right) \times b_{0k}, \tag{21}$$

where N is the total number of clay layers, Th is the random variable for clay layer thickness, $\Pr\left(k-0.5 < Th \le k+0.5\right)$ is the probability that a clay layer will be within 0.5 m of thickness k, and b_{0k} is the thickness that compacted in a clay layer of total thickness k: $b_{0k} = \min\left(2\sqrt{\tau D},\ k\right)$. The total thickness of clay is related to the number and thickness of layers by

$$b_T = N \sum_{k=0}^{30} \Pr\left(k-0.5 < Th \le k+0.5\right) \times k. \tag{22}$$

We were then able to solve for the fraction of total clay that compacts, fr_{b0}, by dividing b_0 by b_T, giving

$$fr_{b0} = \frac{N \sum_{k=0}^{30} \Pr\left(k-0.5 < Th \le k+0.5\right) \times b_{0k}}{N \sum_{k=0}^{30} \Pr\left(k-0.5 < Th \le k+0.5\right) \times k} = \frac{\sum_{k=0}^{30} \Pr\left(k-0.5 < Th \le k+0.5\right) \times b_{0k}}{\sum_{k=0}^{30} \Pr\left(k-0.5 < Th \le k+0.5\right) \times k}. \tag{23}$$

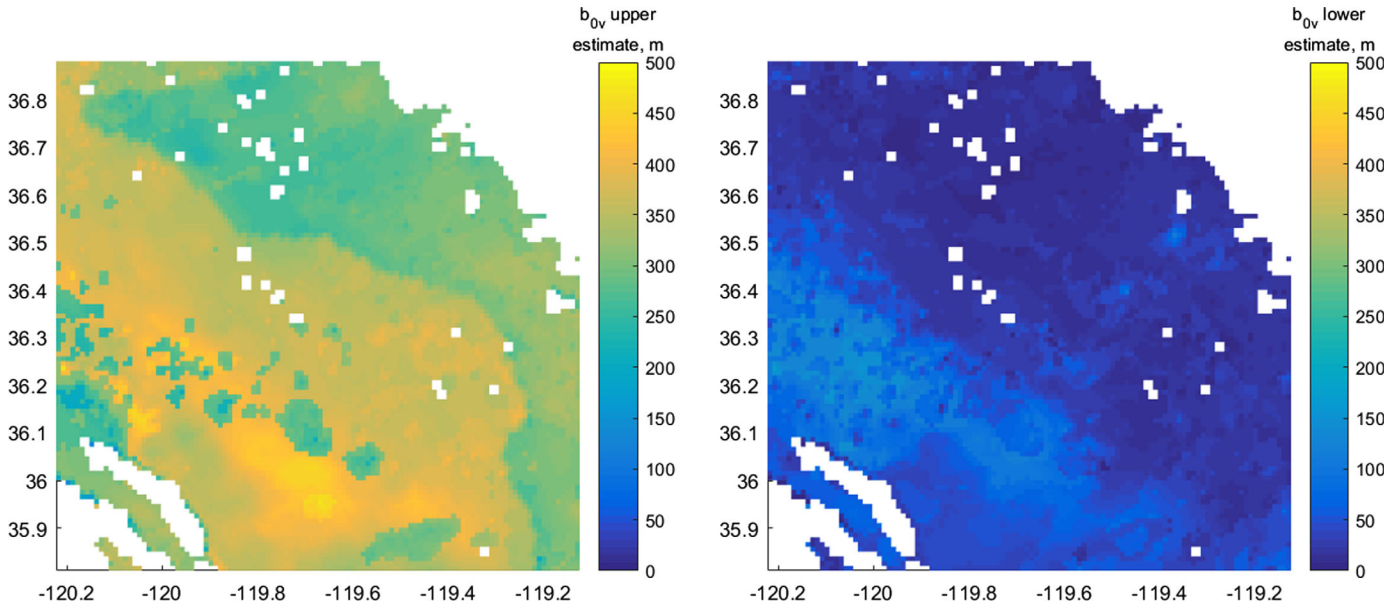

Figure 6. (a) Upper b_{0v} estimate, assumed to be the total amount of clay in the aquifer system as estimated by *Faunt et al.* [2009a]. (b) Lower, more reasonable b_{0v} estimate, based on the total amount of clay as in Figure 6a but also accounting for perforated intervals and an average rate of diffusion for the clay layers. Clay layer thicknesses were estimated using 12 drillers' logs.

From this we determined that for the inelastic case, $fr_{b0}=0.36$. We multiplied fr_{b0} by the clay thickness that is within the perforated intervals to estimate b_0. The resulting b_{0v} estimate ranges from 1 m in the northeast to 142 m in the southwest and is shown in Figure 6b. For the elastic case, we determined $fr_{b0}=0.95$. We multiplied this by the thickness of clay sediments, and added that to the total thickness of sand sediments (assuming that all sand drained during the study period) to estimate b_{0e}. The resulting b_{0e} estimates range from 6 to 549 m, and are shown in Figure S4 of Supporting Information. We consider these estimates of b_{0v} and b_{oe} to be more reasonable than the upper b_{0v} and b_{0e} estimates because these estimates account for additional factors, such as delayed drainage and the bottom of the perforated intervals.

3.4. Computing $\Delta b_{inelastic}$: Analysis and Results

We used the estimates of b_0, S_{ske}, and S_{skv}, and the measurements of Δh_{tot} and Δb_{tot} to compute $\Delta b_{inelastic}$ using equation (18). For S_{ske} we used the estimates for mixed sand and clay systems. Since b_0, S_{ske}, and S_{skv} all have ranges of values, we chose those that correspond to the lower value for $\Delta b_{inelastic}$ (the higher of our b_0 estimates, highest S_{ske}, highest S_{skv}) for what we consider to be the lowest possible estimate. For the second, more reasonable estimate, we chose the lower, more reasonable of our b_0 estimates, and the average values of S_{ske} and S_{skv}. Note that the higher b_0 value corresponds to a lower $\Delta b_{inelastic}$ estimate, because if more clay is undergoing compaction, then a higher fraction of the compaction can be explained by elastic deformation. In these two estimates, we have used a range of estimates for S_{ske}, S_{skv}, and b_0 to account for potential variations in these parameters across our study area.

4. Map of Permanent Compaction: Results and Discussion

The lower estimate of permanent compaction that we obtained (shown in Figure 7a) indicates that the amount of permanent compaction ranges from 0 to 0.66 m, varying spatially throughout the study area. The percentage of the observed compaction that is permanent ranged across our study area from 0 to 100% of the total compaction, with an average of 54% of the observed compaction being permanent. This estimate assumes that all of the clay and sands below the top of the perforated interval in the study area compacted during our study period. Because of delayed drainage due to diffusion, we are confident that the amount of permanent subsidence experienced over our study period is larger than this lower estimate.

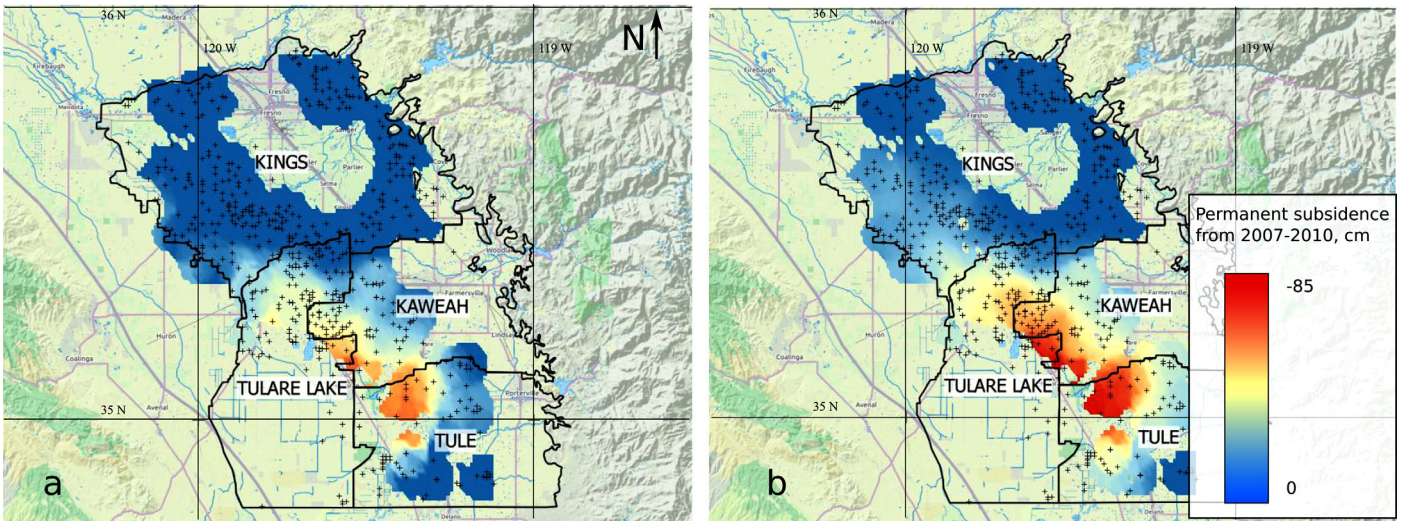

Figure 7. (a) Lower estimate of permanent subsidence (54% of observed subsidence calculated as permanent). (b) Upper, more reasonable estimate of permanent subsidence (98% of observed subsidence calculated as permanent). Wells used in the study are shown as plus symbols.

The upper, more reasonable estimate is shown in Figure 7b and indicates that the amount of permanent compaction ranges from 0 to 0.78 m. The percentage of the observed compaction that is permanent ranges across our study area from 0 to 100% of the total compaction, with an average of 98% of the observed compaction being permanent. This method took into account the estimated perforated intervals, as well as diffusion from clay layers of varying thickness. It assumed that the distribution of clay layer thicknesses is stationary across our study area.

In this method, we estimated the values for the parameters S_{skv}, S_{ske}, and K_v based on values reported by *Sneed* [2001]. Earlier studies have used InSAR time series with co-located head levels to estimate S_{ke} ($=S_{ske}b_0$) [*Reeves et al*., 2011; *Chen et al*., 2016]. In these cases, the head levels were above the preconsolidation head, so the researchers were confident that the deformation was elastic. For the vast majority of our study area, the preconsolidation head was unknown, thus both elastic and inelastic deformation could be occurring. Because of this we were unable to estimate the skeletal-specific storage properties at each well site, but rather relied on previous estimates of geomechanical properties made with extensometer data [*Sneed*, 2001].

There is uncertainty in these estimates, as each of the parameters has a range of reported values. To test the impact of this uncertainty we used the second (more reasonable) method and varied each parameter within the reported range of values. In Figure S4 we show the results of this uncertainty analysis in terms of the resulting fraction of deformation calculated to be permanent. These values range from 95 to 99.5% (within 3% of our best estimate, 98%). Thus, we conclude that varying these parameters does not result in a significant change in the results.

One of the key negative impacts of inelastic deformation is a permanent loss of groundwater storage. Our lower estimate of $\Delta b_{inelastic}$ corresponds to a total loss of groundwater storage of 4.14×10^8 m^3; that volume of groundwater has been permanently removed from the aquifer system. The upper, more reasonable estimate corresponds to a total loss of groundwater storage of 7.48×10^8 m^3. The California Department of Water Resources estimated that the groundwater usage in the planning areas that cover our study area was 1.65×10^{10} m^3 over the time period of our study [*California Department of Water Resources*, 2013]. More spatially detailed groundwater pumping records were not available for our study period. Since our inelastic deformation estimates only cover about half of the planning area, our lower and upper estimates of permanent loss of groundwater storage account for approximately 5 and 9%, respectively, of the total volume of groundwater usage by area over that time period.

The pumped groundwater resulting from compaction of sediments has been referred to as "water of compaction" by *Poland et al*. [1975], who estimated this as a percentage of total pumped groundwater in the Los Banos-Kettleman Hills area (20–60%), as well as the Arvin-Maricopa area (0–40%). Our best estimate

that 9% of pumped groundwater was due to inelastic deformation in our study area differs in two key ways from their estimates. First, we separated inelastic deformation from elastic deformation, a distinction not made by *Poland et al*. [1975]. Second, our estimate represents a regionally averaged value because we did not have detailed groundwater pumping data over our study area, while theirs represents a spatially varying map. Since our estimate included areas that experienced very little inelastic deformation, as well as areas that experienced a high degree of inelastic deformation, it is likely that the percentage of pumped groundwater that was due to inelastic deformation of sediments over our study period was much higher than 9% toward the southwest part of our study area, where inelastic deformation was highest.

5. Validation

To validate this new method of computing permanent loss of groundwater storage, we compared our results with a recent study of *Faunt et al*. [2016] which analyzed InSAR data and changes in hydraulic head over the same study area from 2008 to 2010. They analyzed historic groundwater levels, where available, over the southern San Joaquin Valley and found that in most cases these wells had dropped below their preconsolidation head, resulting in inelastic deformation, from Spring 2008 to the date of publishing. This study builds on their work by quantifying the degree of inelastic deformation even in areas that don't have historic well data, and in general agrees with their observation that significant inelastic deformation occurred during this time period.

To further validate this method, we did a quantitative analysis using a traditional method that uses the preconsolidation head to estimate inelastic deformation. We analyzed all wells in our study area that had at least eight measurements taken from 2007 to 2010, and at least 65 measurements taken over a period of at least 40 years prior to 2007. Having a relatively high measurement frequency gave us more confidence in estimating the preconsolidation head, although there is still uncertainty in this estimate. The above criteria resulted in a data set of 28 wells. We removed 10 wells from this data set due to an abundance of noisy measurements, thus we were left with 18 wells. One of the wells, with its collocated InSAR-derived ground displacement, used in this analysis is shown in Figure S6 of Supporting Information. At the remaining 18 wells, we calculated the difference between the minimum head from 2007 to 2010 and the pre-2007 preconsolidation head. We refer to this value as $\Delta h_{inelastic}$. A positive value of $\Delta h_{inelastic}$ indicates the head from 2007 to 2010 did not drop below the preconsolidation head, while a negative value indicates that it did drop below the preconsolidation head.

The 18 calculated values of $\Delta h_{inelastic}$ ranged from -7.1 to 2.1 m, with an average of -1.8 m, meaning on average the head dropped 1.8 m below the preconsolidation head. We also calculated the drop in head at each well in the elastic range (above the preconsolidation head). We refer to this as $\Delta h_{elastic}$. These values ranged from -1.5 to -11.4 m, with an average of -6.6 m.

We used equation (23) and the methods outlined in section 3.3 to calculate b_{0v} and b_{0e}, and equations (8) and (9) to calculate $\Delta b_{inelastic}$ and $\Delta b_{elastic}$. Summing the two results in an estimate of Δb_{tot}. Calculating these variables required estimates of K_v, S_{skv}, and S_{ske}. We used the average values for these parameters from those reported by *Sneed* [2001], as described in section 2.1. We divided the sum of $\Delta b_{inelastic}$ by the sum of Δb_{tot} over all 18 wells to estimate the percent of deformation that was inelastic, or permanent: 89%. This is the estimated percentage of deformation that was permanent at these specific wells. We then estimated the percent of deformation that was permanent at these wells with the new method as described in section 3. We used the upper, more reasonable estimate for comparison, and the resulting estimate was 91%. Since these two methods arrived at such similar outcomes, we consider this a validation that our method can effectively estimate inelastic deformation without prior knowledge of the preconsolidation head.

6. Conclusions

We estimated the amount of permanent compaction that occurred from June 2007 to December 2010 using a combination of InSAR deformation measurements, head measurements, and constitutive geomechanical equations. Because of uncertainty in S_{skv}, S_{ske}, and b_0, we made two estimates, a lower estimate and an upper, more reasonable estimate, to obtain the range of inelastic deformation. Our results suggest that significant permanent compaction occurred during our study period. The amount of permanent

subsidence was estimated to be at least 54% of the total subsidence measured. Our more reasonable estimate was that 98% of the total subsidence measured was permanent. These two estimates correspond to a permanent loss in groundwater storage of 4.14×10^8 m^3 and 7.48×10^8 m^3, respectively. While this is just a small fraction of the total water stored underground in this area, water extracted from clays during inelastic deformation is an important safeguard for times of drought that, once removed, cannot be replenished.

This study highlights a region that is experiencing significant inelastic deformation—the subsidence bowl that spans the northeast corner of Tulare Lake subbasin, and the western edges of Kaweah and Tule subbasins. Because of high clay content, this region is likely to experience inelastic deformation again when groundwater pumping and limited recharge occur during times of drought.

Our approach outlined in this study is a useful one for groundwater managers because it does not require the time and resource-intensive development and calibration of a groundwater model. It also does not require an extensive history of head levels over the study area to compute the preconsolidation head. This is advantageous for an area like the San Joaquin Valley, where most water level data are from irrigation wells and have some data quality issues, so an estimate of the preconsolidation head would have a high degree of uncertainty. It also is straightforward to update using additional head and InSAR data as they are acquired. Our method does require significant knowledge of the clay content of the aquifer system. In the San Joaquin Valley, the geologic model of *Faunt et al*. [2009a] is very useful for this purpose. Applying this method to another area would require the development of a geologic model that estimates clay content, as well as information about the distribution of clay layer thicknesses, and estimates for the parameters K_v, S_{skv}, and S_{ske}.

Acknowledgments

We would like to thank the reviewers, whose helpful comments and insights have greatly improved this manuscript. We would also like to thank Michelle Sneed (USGS) for her valuable feedback related to aquifer compaction studies in the San Joaquin Valley. Finally, we would like to thank Mary Scruggs from the California Department of Water Resources for discussions on the data quality of water level records, and general groundwater pumping observations in the San Joaquin Valley. This research was initiated with funding to R. Knight from the S.D. Bechtel Jr. Foundation and then continued with funding to R. Knight and H. Zebker from the NASA Terrestrial Hydrology Program (grant NNX12AP59G). R. Smith was supported by a National Science Foundation Fellowship (grant DGE-114747). Part of this work was carried out at the Jet Propulsion Laboratory, California Institute of Technology, under contract with NASA. The textural model, water level data, GPS data, hydrologic properties, and geomechanical properties have been cited throughout the paper and are publicly available. The SAR data used for processing interferograms are available from the Alaska Satellite Facility following registration. The data sets developed by the authors, i.e., the estimates of inelastic deformation, and the thickness of sediment undergoing inelastic and elastic deformation, are available upon request from the corresponding author.

References

Bell, J. W., F. Amelung, A. Ferretti, M. Bianchi, and F. Novali (2008), Monitoring aquifer-system response to groundwater pumping and artificial recharge, *First Break*, *26*(8), 85–91, doi:10.1029/2007WR006152.

Berardino, P., G. Fornaro, R. Lanari, and E. Sansosti (2002), A new algorithm for monitoring localized deformation phenomena based on small baseline differential SAR interferograms, *IEEE Int. Geosci. Remote Sens. Symp.*, *2*(11), 2375–2383, doi:10.1109/IGARSS.2002.1025900.

California Department of Water Resources (2013), *California Water Plan: Investing in Innovation and Infrastructure*. Tulare Lake Hydrologic Region, vol. 2, South Central Regional Office, Fresno, Calif.

California Department of Water Resources (2007), Integrated water flow model, IWFM v4.0, theoretical document.

Chaussard, E., R. Bürgmann, M. Shirzaei, E. J. Fielding, and B. Baker (2014), Predictability of hydraulic head changes and characterization of aquifer-system and fault properties from InSAR-derived ground deformation, *J. Geophys. Res. Solid Earth*, *119*, 6572–6590, doi:10.1002/2014JB011266.

Chen, C. W., and H. A. Zebker (2001), Two-dimensional phase unwrapping with use of statistical models for cost functions in nonlinear optimization, *J. Opt. Soc. Am. A*, *18*(2), 338, doi:10.1364/JOSAA.18.000338.

Chen, J., R. Knight, H. A. Zebker, and W. A. Schreüder (2016), Confined aquifer head measurements and storage properties in the San Luis Valley, Colorado, from spaceborne InSAR observations, *Water Resour. Res.*, *52*, 3623–3636, doi:10.1002/2015WR018466.

Farr, T. G., and Z. Liu (2015), Monitoring subsidence associated with groundwater dynamics in the Central Valley of California using interferometric radar, in *Remote Sensing of the Terrestrial Water Cycle, Geophys. Monogr.*, vol. 206, edited by V. Lakshmi, AGU, Washington, D. C.

Faunt, C. C., K. Belitz, and R. T. Hanson (2009a), Development of a three-dimensional model of sedimentary texture in valley-fill deposits of Central Valley, California, USA, *Hydrogeol. J.*, *18*(3), 625–649, doi:10.1007/s10040-009-0539-7.

Faunt, C. C., R. T. Hanson, K. Belitz, W. Schmid, S. P. Predmore, D. L. Rewis, and K. McPherson (2009b), *Groundwater Availability of the Central Valley Aquifer, California*., U.S. Geol. Surv. Prof. Pap., 1776, 225 pp.

Faunt, C. C., M. Sneed, J. Traum, and J. T. Brandt (2016), Water availability and land subsidence in the Central Valley, California, USA, *Hydrogeol. J.*, *24*, 1–10, doi:10.1007/s10040-015-1339-x.

Fetter, C. W. (2001), *Applied Hydrogeology*, vol. 3, Prentice Hall, Englewood Cliffs, N. J.

Galloway, D., and F. S. Riley (1999), San Joaquin Valley, California: Largest human alteration of the Earth's surface, *U.S. Geol. Surv. Circ.*, *1182*, 23–34.

Helm, D. C. (1975), One-dimensional simulation of aquifer system compaction near Pixley, California: 1. Constant parameters, *Water Resour. Res.*, *11*(3), 465–478, doi:10.1029/WR011i003p00465.

Hoffmann, J., S. A. Leake, D. L. Galloway, and A. Wilson (2003a), MODFLOW-2000 ground-water model—User guide to the subsidence and Aquifer-System Compaction (SUB) package, *U.S. Geol. Surv. Open File Rep.*, *03*, 46.

Hoffmann, J., D. L. Galloway, and H. A. Zebker (2003b), Inverse modeling of interbed storage parameters using land subsidence observations, Antelope Valley, California, *Water Resour. Res.*, *39*(2), 1031, doi:10.1029/2001WR001252.

Jacob, C. E. (1940), The flow of water in an elastic artesian aquifer, *Eos Trans. AGU*, *21*, 574–586, doi:10.1029/TR021i002p00574.

Leake, S. A. (1990), Interbed storage changes and compaction in models of regional groundwater flow, *Water Resour. Res.*, *26*(9), 1939–1950, doi:10.1029/WR026i009p01939.

Leake, S. A., and D. L. Galloway (2007), MODFLOW ground-water model: User guide to the subsidence and aquifer-system compaction package (SUB-WT) for water-table aquifers, *U.S. Geol. Surv. Tech. Methods*, *6-A23*, 5 pp.

Madsen, S. N., and H. A. Zebker (1998), Imaging radar interferometry, in *Principles and Applications of Imaging Radar, Manual of Remote Sensing*, edited by F. M. Henderson and A. J. Lewis, vol. 2, chap. 6, pp. 359–380, John Wiley, New York.

Page, R. W. (1986), Geology of the fresh ground-water basin, Central Valley, California, with texture maps and sections: U.S. Geological Survey Professional Paper 1401-C, 54 pp.

Poland, J. F., and G. H. Davis (1969), Land-surface subsidence due to the withdrawal of fluids, *Rev. Eng. Geol.*, *2*, 187–270.

Poland, J. F., B. E. Lofgren, R. L. Ireland, and R. G. Pugh (1975), Land subsidence in the San Joaquin Valley, California, as of 1972, *U.S. Geol. Surv. Prof. Pap.*, *437-H*, 77 pp.

Reeves, J. A., R. Knight, H. A. Zebker, W. A. Schreüder, P. Shanker Agram, and T. R. Lauknes (2011), High quality InSAR data linked to seasonal change in hydraulic head for an agricultural area in the San Luis Valley, Colorado, *Water Resour. Res.*, *47*, W12510, doi:10.1029/2010WR010312.

Riley, F. S. (1969), Analysis of borehole extensometer data from central California, *Int. Assoc. Sci. Hydrol. Publ.*, 89, 423–431.

Riley, F. S. (1998), Mechanics of aquifer systems—The scientific legacy of Dr. Joseph F. Poland, in *Land Subsidence Case Studies and Current Research: Proceedings of the Dr. Joseph F. Poland Symposium on Land Subsidence*, *Assoc. Eng. Geol. Spec. Publ.*, vol. 8, edited by J. W. Borchers, pp. 13–27, Star Publishing Company, Belmont, Calif.

Rosen, P., S. Hensley, I. Joughin, F. K. Li, S. Madsen, E. Rodriguez, and R. M. Goldstein (2000), Synthetic aperture radar interferometry, *Proc. IEEE*, *88*(3), 333–382, doi:10.1109/5.838084.

Samsonov, S. (2010), Topographic correction for ALOS PALSAR interferometry, *IEEE Trans. Geosci. Remote Sens.*, *48*(7), 3020–3027, doi:10.1109/TGRS.2010.2043739.

Sansosti, E., F. Casu, M. Manzo, and R. Lanari (2010), Space-borne radar interferometry techniques for the generation of deformation time series: An advanced tool for Earth's surface displacement analysis, *Geophys. Res. Lett.*, *37*(20), 1–9, doi:10.1029/2010GL044379.

Scott, R. F. (1963), Principles of Soil Mechanics, Addison-Wesley Pub. Co., 550 pp., Palo Alto, Calif.

Sneed, M. (2001), Hydraulic and mechanical properties affecting ground-water flow and aquifer-system compaction, San Joaquin Valley, California, *U.S. Geol. Surv. Open File Rep.*, *01–35*, pp. 5–17.

Terzaghi, K. (1925), Structure and volume of voids in soils, translated from Erdbaummechanik auf Bodenphysikalischer Grundlage, in *From Theory to Practice in Soil Mechanics*, John Wiley, New York.

Williamson, A. K., D. E. Prudic, and L. A. Swain (1989), Ground-water flow in the Central Valley, California: Regional aquifer-system analysis—Central Valley, California, *U.S. Geol. Surv. Prof. Pap.*, *1401-D*, pp. 33–37.